

EXAFS Study of Aqueous Zr^{IV} and Th^{IV} Complexes in Alkaline CaCl₂ Solutions: Ca₃[Zr(OH)₆]⁴⁺ and Ca₄[Th(OH)₈]⁴⁺

B. Brendebach,* M. Altmaier, J. Rothe, V. Neck, and M. A. Denecke

Forschungszentrum Karlsruhe, Institut für Nukleare Entsorgung, P.O. Box 3640, D-76021 Karlsruhe, Germany

Received February 17, 2007

A hitherto unknown type of aqueous complex, ternary Ca–M^{IV}–OH complexes (M = Zr and Th), causes unexpectedly high solubilities of zirconium(IV) and thorium(IV) hydrous oxides in alkaline CaCl₂ solutions (pH_c = 10–12, [CaCl₂] > 0.05 mol·L⁻¹, and pH_c = 11–12, [CaCl₂] > 0.5 mol·L⁻¹, respectively). The dominant aqueous species are identified as Ca₃[Zr(OH)₆]⁴⁺ and Ca₄[Th(OH)₈]⁴⁺ and characterized by extended X-ray absorption fine structure (EXAFS) spectroscopy. The number of OH⁻ ligands in the first coordination sphere detected by EXAFS, N_O = 6 (6.6 ± 1.2) for Zr and N_O = 8 (8.6 ± 1.2) for Th, are consistent with the observed slopes of 2 and 4 in the solubility curves log [M]_{tot} vs pH_c. The presence of polynuclear hydrolysis species and the formation of chloride complexes can be excluded. EXAFS spectra clearly show a second coordination shell of calcium ions. The [Zr(OH)₆]²⁻ and [Th(OH)₈]⁴⁻ complexes with an unusually large number of OH⁻ ligands are stabilized by the formation of associates or ion pairs with Ca²⁺ ions. The number of neighboring Ca²⁺ ions around the [Zr(OH)₆]²⁻ and [Th(OH)₈]⁴⁻ units is determined to be N_{Ca} = 3 (2.7 ± 0.6) at a distance of R_{Zr–Ca} = 3.38 ± 0.02 Å and N_{Ca} = 4 (3.8 ± 0.5) at a distance of R_{Th–Ca} = 3.98 ± 0.02 Å. The Ca₃[Zr(OH)₆]⁴⁺ and Ca₄[Th(OH)₈]⁴⁺ complexes have first (M–O) and second (M–Ca) coordination spheres with the Ca²⁺ ions bound to coordination polyhedra edges.

1. Introduction

The solubility and aqueous speciation of zirconium and thorium in chloride solutions is of particular interest for the storage of nuclear waste in underground salt mines, e.g., in the Waste Isolation Pilot Plant in New Mexico or the Asse salt mine in Germany. Because the corrosion of cementitious waste forms can lead to alkaline CaCl₂ solutions, we study the solubility of zirconium(IV) and thorium(IV) oxyhydroxide precipitates, which may be called either hydrous oxide, MO₂·xH₂O(s), or hydroxide, M(OH)₄(s), as a function of pH at different NaCl and CaCl₂ concentrations. Because of the formation of solid calcium hydroxide or hydroxychlorides, the pH range in 0.1–4.5 M CaCl₂ solutions is limited to values below 12. Numerous solubility studies with ZrO₂·xH₂O(s), ThO₂·xH₂O(s), and the hydrous oxides of other tetravalent actinides in NaCl–NaOH, NaClO₄–NaOH, LiOH, KOH, or NaOH solutions up to pH 14 show no indication of the formation of anionic hydroxide complexes M(OH)_n⁴⁻ⁿ with n > 4 (cf. discussions in recent reviews^{1–3}). The

solubilities measured after ultrafiltration (pore size 1.5–2 nm) or ultracentrifugation in carbonate-free solutions at pH 5–13 are very low and at a constant concentration level (log [Th] = -8.5 ± 0.6,^{1,4} and log [Zr] = -7.4 ± 0.6^{3,5} or -7.8 ± 0.6⁶). These concentrations are usually described by equilibria between MO₂·xH₂O(s) or M(OH)₄(s) and neutral aqueous complexes M(OH)₄(aq) or M_n(OH)_{4n}(aq). An increase of the solubility due to the formation of Zr(OH)₅⁻ or Zr(OH)₆²⁻ has been observed only at very high hydroxide concentrations, e.g., in 1–10 M NaOH.^{3,5,7,8}

* To whom correspondence should be addressed. E-mail: boris.brendebach@ine.fzk.de.

(1) Neck, V.; Kim, J. I. *Radiochim. Acta* **2001**, *89*, 1–16.

(2) Guillaumont, R.; Fanghänel, Th.; Fuger, J.; Grenthe, I.; Neck, V.; Palmer, D. A.; Rand, M. H. *OECD, NEA-TDB, Chemical Thermodynamics Vol. 5. Update on the Chemical Thermodynamics of Uranium, Neptunium, Plutonium, Americium and Technetium*; Elsevier: Amsterdam, The Netherlands, 2003.

(3) Brown, P. L.; Curti, E.; Grambow, B.; Ekberg, C. *OECD, NEA-TDB, Chemical Thermodynamics Vol. 8. Chemical Thermodynamics of Zirconium*; Elsevier: Amsterdam, The Netherlands, 2005.

(4) Neck, V.; Müller, R.; Bouby, M.; Altmaier, M.; Rothe, J.; Denecke, M. A.; Kim, J. I. *Radiochim. Acta* **2002**, *90*, 485–494.

(5) Ekberg, C.; Källvenius, G.; Albinsson, Y.; Brown, P. L. *J. Solution Chem.* **2004**, *33*, 47–79.

(6) Altmaier, M.; Neck, V.; Fanghänel, Th., to be published and to be presented at the conference Migration '07.

(7) Sheka, I. A.; Pevzner, T. V.; Russ, J. *Inorg. Chem.* **1960**, *5*, 1119–1121.

Contrary to these results, the solubilities measured in our extensive studies with zirconium(IV) and thorium(IV) hydrous oxides at $\text{pH}_c = 10\text{--}12$ in CaCl_2 solutions are unexpectedly high.⁶ The Zr^{IV} and Th^{IV} concentrations are above $10^{-3} \text{ mol}\cdot\text{L}^{-1}$ and hence sufficiently high to investigate the saturated solutions by extended X-ray absorption fine structure (EXAFS) spectroscopy. The stoichiometries of the dominant aqueous complexes can also be derived from the dependencies of the solubility data on pH and CaCl_2 concentration. Possible structures of these complexes are derived and compared with previous EXAFS data for the aqua ion $\text{Th}^{4+}(\text{aq})$, crystalline oxides $\text{ZrO}_2(\text{cr})$ and $\text{ThO}_2(\text{cr})$, and polymeric/colloidal oxyhydroxide species of Zr^{IV} and Th^{IV}.^{4,9–13} The present paper is primarily focused on the results and discussion of our EXAFS measurements. The comprehensive sets of solubility experiments performed with hydrous oxides of Zr^{IV}, Th^{IV}, and Pu^{IV} in dilute to concentrated CaCl_2 solutions (and for comparison also in NaCl and $\text{Ca}(\text{ClO}_4)_2$ solutions) will be published in a forthcoming paper.⁶ Part of our solubility data is briefly discussed as background to the EXAFS study.

2. Experimental Section

2.1. Solubility Studies. Solid precipitates of $\text{ZrO}_2\cdot x\text{H}_2\text{O}(\text{s})$ and $\text{ThO}_2\cdot x\text{H}_2\text{O}(\text{s})$ are prepared by the slow addition of 0.1 M NaOH (carbonate-free, Baker) to approximate 0.02 M solutions of $\text{Th}(\text{NO}_3)_4\cdot 6\text{H}_2\text{O}$ (Merck) and $\text{ZrOCl}_2\cdot x\text{H}_2\text{O}$ (Aldrich). The precipitates are washed several times with water and stored for about 2 weeks. The Th^{IV} precipitate is X-ray amorphous, while the powder diffraction pattern of the Zr^{IV} precipitate shows the most intense peaks of monoclinic $\text{ZrO}_2(\text{cr})$ as weak broad bands. Appropriate amounts of the zirconium(IV) or thorium(IV) hydrous oxides are suspended in 10–50 mL of the matrix solution (see below) and equilibrated for 14–198 days in polyethylene vials. The experiments are performed at 22 ± 2 °C in an argon glovebox.

The matrix solutions for the different series of solubility experiments in 0.1, 0.2, 0.5, 1.0, 2.0, and 4.5 M CaCl_2 are prepared with $\text{CaCl}_2\cdot 2\text{H}_2\text{O}$ (p.a., Merck) and ultrapure water purged with argon. Matrix solutions at maximum pH are obtained by equilibration with solid $\text{Ca}(\text{OH})_2$ (p.a., Merck) for about 1 week and subsequent ultrafiltration. In 4.5 M CaCl_2 , the solid calcium hydroxide transforms into calcium hydroxychlorides $\text{Ca}_4(\text{OH})_6\text{Cl}_2\cdot 13\text{H}_2\text{O}(\text{cr})$ and/or $\text{Ca}_2(\text{OH})_2\text{Cl}_2\cdot \text{H}_2\text{O}(\text{cr})$ ¹⁴ within a few days. The zirconium and thorium concentrations are determined after 10 kD (ca. 1.5 nm) ultrafiltration or ultracentrifugation (Beckman XL-90; mean relative centrifugal force = approximately $5 \times 10^5 g$) by ICP-MS (ELAN 6100, Perkin-Elmer). The molar H^+ concentrations ($-\log [\text{H}^+] = \text{pH}_c$) are determined with combined pH electrodes

Table 1. Summary of EXAFS Samples

ID	sample description
Zr-a	8.3×10^{-4} M Zr ^{IV} in 0.5 M CaCl_2 , $\text{pH}_c = 12.0$
Zr-b	1.5×10^{-3} M Zr ^{IV} in 1.0 M CaCl_2 , $\text{pH}_c = 11.9$
Zr-c	1.7×10^{-3} M Zr ^{IV} in 2.0 M CaCl_2 , $\text{pH}_c = 11.6$
Zr-d	5.9×10^{-3} M Zr ^{IV} in 2.0 M CaCl_2 , $\text{pH}_c = 12.0$
Th-e	4.3×10^{-3} M Th ^{IV} in 4.5 M CaCl_2 , $\text{pH}_c = 12.2$

(type ROSS, Orion) calibrated against CaCl_2 standard solutions containing 0.001–0.1 M HCl . Details are given in a previous paper for analogous pH measurements in NaCl and MgCl_2 solutions.¹⁵

2.2. EXAFS Measurements. Liquid samples prepared for the EXAFS measurements are taken from the CaCl_2 solutions saturated with $\text{ZrO}_2\cdot x\text{H}_2\text{O}(\text{s})$ or $\text{ThO}_2\cdot x\text{H}_2\text{O}(\text{s})$. Filtered aliquots are filled in 2 mL polyethylene vials. A summary of the investigated samples is listed in Table 1.

Measurements are performed at the INE-Beamline for Actinide Research¹⁶ at the Ångströmquelle Karlsruhe (ANKA), Forschungszentrum Karlsruhe, Karlsruhe, Germany, with the storage ring operating at 2.5 GeV and electron currents ranging from 180 to 100 mA. The X-ray double-crystal monochromator is equipped with a pair of Ge(422) crystals ($2d = 2.304$ Å). Suppression of higher harmonics is achieved by the rhodium-coated mirrors in the INE-Beamline optics. Constant incoming intensity in each scan is achieved by detuning the second crystal from the parallel alignment to 60% maximum beam intensity using a MOSTAB piezoactuator, equipped with a feedback control loop to keep the intensity in the first ionization chamber constant. Spectra are recorded in fluorescence mode by registering the Zr $K\alpha_{1,2}$ or Th $L\alpha_{1,2}$ fluorescence radiation at approximately 15.7 or 12.9 keV, respectively, as a function of the incident photon energy using a 5-pixel energy-dispersive solid-state germanium detector (Canberra LEGe). Five to eight spectra are recorded and averaged for each sample to improve the signal-to-noise ratio. The spectrum of a zirconium foil is recorded simultaneously for energy calibration, setting the first derivative in its XANES to 17.998 keV.¹⁷

EXAFS data analysis is based on standard least-square-fitting techniques¹⁸ using the UWXAFS suite of programs.¹⁹ Within the autobk program, the atomic background $\mu_0(E)$ is optimized with respect to spurious contributions in the k^3 -weighted Fourier-transformed data below 1 Å, which corresponds to about half of the nearest-neighbor distance. The maximum of the most intense absorption feature, the so-called white line, is set to the ionization energy, E_0 , which serves as the origin for generating k values. The EXAFS functions, $\chi(k)$, are k^3 -weighted and Fourier-transformed using a Hanning window with $\Delta k = 0.2$ Å⁻¹ sills. In the case of the zirconium spectra, a k range of 2.4–13.5 Å⁻¹ is Fourier-transformed; a k range of 2.7–14 Å⁻¹ is used for the thorium sample. Fitting of the metric parameters, coordination numbers N_i , distances to the neighboring atoms R_i , and mean-square displacements or Debye–Waller factors σ_i^2 , is performed in R space over a range of 1.1–3.4 Å for the zirconium data and 1.6–3.9 Å for thorium using the FEFFIT program. Backscattering amplitude and phase shift functions are calculated with help of the FEFF8.2

- (8) Adair, J. H.; Denkwicz, R. P.; Arriagada, F. J.; Osseo-Assare, K. *Ceram. Trans.* **1987**, *1*, 135–145.
 (9) Moll, H.; Denecke, M. A.; Jalilehvand, F.; Sandström, M.; Grenthe, I. *Inorg. Chem.* **1999**, *38*, 1795–1799.
 (10) Rothe, J.; Denecke, M. A.; Neck, V.; Müller, R.; Kim, J. I. *Inorg. Chem.* **2002**, *41*, 249–258.
 (11) Cho, H. R.; Walther, C.; Rothe, J.; Neck, V.; Denecke, M. A.; Dardenne, K.; Fanghänel, Th. *Anal. Bioanal. Chem.* **2005**, *383*, 28–40.
 (12) Walther, C.; Rothe, J.; Fuss, M.; Büchner, S.; Koltsov, S.; Bergmann, T. *Anal. Bioanal. Chem.* **2007**, *388*, 409–431.
 (13) Hagfeldt, C.; Kessler, V.; Persson, I. *Dalton Trans.* **2004**, *14*, 2142–2151.
 (14) Harvie, C. F.; Møller, N.; Weare, J. H. *Geochim. Cosmochim. Acta* **1984**, *48*, 723–751.

- (15) Altmaier, M.; Metz, V.; Neck, V.; Müller, R.; Fanghänel, Th. *Geochim. Cosmochim. Acta* **2003**, *67*, 3595–3601.
 (16) Denecke, M. A.; Rothe, J.; Dardenne, K.; Blank, H.; Hormes, J. *Phys. Scr.* **2005**, *T115*, 1001–1003.
 (17) Bearden, J. A.; Burr, A. F. *Rev. Mod. Phys.* **1967**, *39*, 125–142.
 (18) Koningsberger, D. C.; Prins, R. *X-ray Absorption: Principles, Applications, Techniques of EXAFS, SEXAFS and XANES*; John Wiley & Sons: New York, 1988.
 (19) Stern, E. A.; Newville, M.; Ravel, B.; Yacoby, Y.; Haskel, D. *Physica B* **1995**, *208–209*, 117–120.

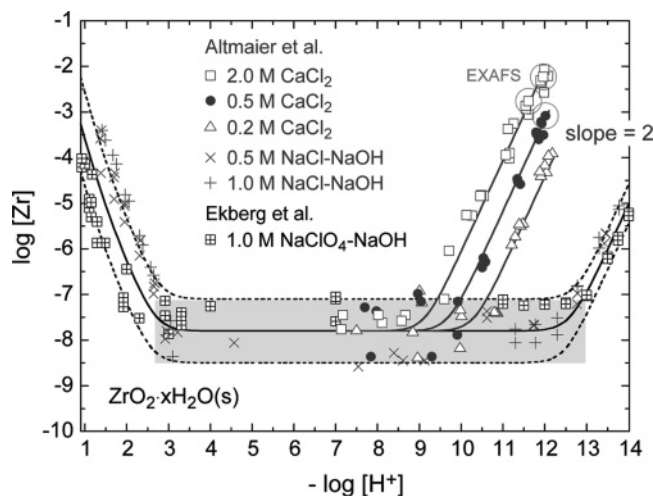


Figure 1. Solubility of $\text{ZrO}_2 \cdot x\text{H}_2\text{O}(\text{s})$ in NaClO_4 , NaCl , and CaCl_2 solutions at 20–25 °C. The solid lines calculated for alkaline CaCl_2 solutions are based on $\log K_{s,6-3}^\circ = 0.7 \pm 0.3$; the SIT is used for ionic strength corrections. Dashed lines represent upper and lower limits. Shaded gray areas are regions of constant zirconium concentration.

program.²⁰ The amplitude reduction factor, $S_0^{2,21}$ is held constant at unity in all fits. Shifts of the ionization potential, ΔE_0 , are allowed to vary independently for each shell, as suggested in the FEFFIT documentation.²²

3. Results and Discussion

3.1. Solubility of Zirconium(IV) Hydrated Oxide. Figure 1 shows solubility data measured with zirconium(IV) hydrated oxide in 1.0 M NaClO_4 ⁵ and in 0.5 and 1.0 M NaCl over the entire pH range studied. The differences between the curves are typical for differences in the degree of crystallinity or particle size due to somewhat different preparation and aging conditions. These effects are usually larger than the differences due to the different ionic media and ionic strengths in these studies. In the range $\text{pH}_c = 3$ –13 in NaCl or NaClO_4 media, the zirconium concentration is at a constant level. The scatter of the data at these low concentrations arises from analytical difficulties, insufficient separation of colloidal species, and/or sorption effects during phase separation. At $\text{pH}_c > 13$, the solubility curves ($\log [\text{Zr}]$ vs pH_c) show a distinct increase with a slope of 2 due to the formation of the complex $\text{Zr}(\text{OH})_6^{2-}$.³ In a CaCl_2 solution, this solubility increase with slope 2 is more pronounced and already observed at significantly lower pH_c values in the range 10–12. The solubility in 0.5 and 1.0 M NaCl/NaOH solutions is not markedly different from that in 1.0 M $\text{NaClO}_4/\text{NaOH}$ but orders of magnitude lower than those in CaCl_2 solutions with similar chloride concentrations. This indicates that the solubility increase is not caused by complex formation with chloride ions but by strong interaction with Ca^{2+} as a result of either ion association or ion-pair formation. This assumption is further corroborated by additional solubility experiments in perchlorate media. The

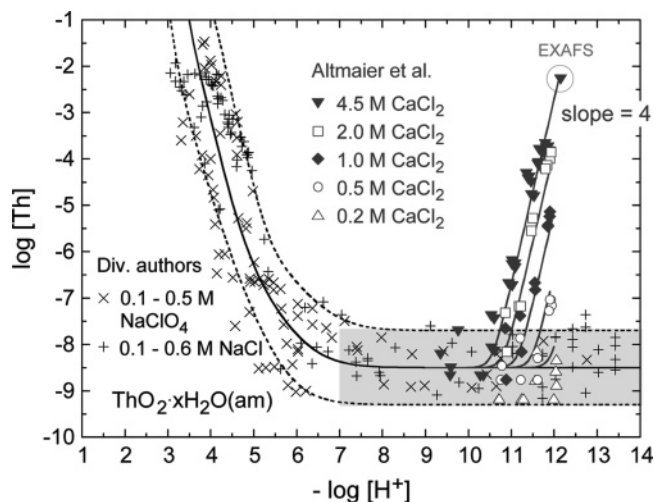


Figure 2. Solubility of $\text{ThO}_2 \cdot x\text{H}_2\text{O}(\text{s})$ in NaClO_4 , NaCl , and CaCl_2 solutions at 17–25 °C. The experimental data in NaClO_4 and NaCl media and the corresponding calculation are taken from ref 4 and references cited therein.^{23–28} The solid lines calculated for alkaline CaCl_2 solutions are based on $\log K_{s,8-4}^\circ = 1.8 \pm 0.5$; the SIT is used for ionic strength corrections. Dashed lines represent upper and lower limits. Shaded gray areas indicate regions of constant thorium concentration.

ClO_4^- anion is generally considered noncomplexing, but the zirconium concentrations measured after 14 and 27 days in 0.2 and 1.0 M $\text{Ca}(\text{ClO}_4)_2$ ⁶ are close to the solubilities observed in 0.2 and 1.0 M CaCl_2 .

3.2. Solubility of Thorium(IV) Hydrated Oxide. The solubility of thorium(IV) hydrated oxide in 0.1–0.5 M NaCl or NaClO_4 solutions is shown as crosses in Figure 2. The calculated solubility and uncertainty range for the experimental data under these conditions is taken from Neck et al.;⁴ the experimental data are taken from the same paper and the references cited therein.^{23–28} In neutral and alkaline solution ($\text{pH}_c = 6$ –14), the solubility remains constant at $\log [\text{Th}] = -8.5 \pm 0.6$. The experimental data in 0.2 M CaCl_2 and those at higher CaCl_2 concentrations and $\text{pH}_c < 11$ fall also into this range. However, the thorium concentrations measured in 0.5, 1.0, 2.0, and 4.5 M CaCl_2 in the range $\text{pH}_c = 11$ –12 show a steep increase and a systematic dependence on the CaCl_2 concentration. Because the thorium concentrations measured after a few days are not markedly different from those measured after 3–6 months, the initial $\text{Th}(\text{OH})_4(\text{am})$ is the solubility-controlling solid phase in these experiments. (The occurrence of a solid transformation would cause a decrease in solubility with time.) Accordingly, the observed dependence on pH_c (slope 4 for $\log [\text{Th}]$ vs pH_c) indicates the formation of a thorium(IV) hydroxide complex with eight OH^- ligands. This is an unexpected result because the available data in a NaCl and NaClO_4 solution and in lithium and tetramethylammonium hydroxide solutions up

(20) Ankudinov, A. L.; Ravel, B.; Rehr, J. J.; Conradson, S. D. *Phys. Rev. B* **1998**, *58*, 7565–7576.

(21) Lee, P. A.; Citrin, P. H.; Eisenberger, P.; Kincaid, B. M. *Rev. Mod. Phys.* **1981**, *53*, 769–806.

(22) Newville, M. *FEFFIT Documentation*, available online.

(23) Ryan, J. L.; Rai, D. *Inorg. Chem.* **1987**, *26*, 4140–4142.

(24) Nabivanets, B. I.; Kudritskaya, L. N. *Ukr. Khim. Zh.* **1964**, *30*, 891–895.

(25) Moon, H. C. *Bull. Korean Chem. Soc.* **1989**, *10*, 270–272.

(26) Felmy, A. R.; Rai, D.; Mason, M. J. *Radiochim. Acta* **1991**, *55*, 177–185.

(27) Östholts, E.; Bruno, J.; Grenthe, I. *Geochim. Cosmochim. Acta* **1994**, *58*, 613–623.

(28) Rai, D.; Moore, D. A.; Oakes, C. S.; Yui, M. *Radiochim. Acta* **2000**, *88*, 297–306.

Table 2. Ion Interaction (SIT) Coefficients, ϵ_{ij} , Used

<i>i</i>	<i>j</i>	ϵ_{ij} (kg·mol ⁻¹)
H ⁺	Cl ⁻	0.12 ± 0.01 ^a
Na ⁺	Cl ⁻	0.03 ± 0.01 ^a
Ca ²⁺	Cl ⁻	0.14 ± 0.01 ^a
OH ⁻	Na ⁺	0.04 ± 0.01 ^a
OH ⁻	Ca ²⁺	-0.45 ± 0.03 ^c
Zr(OH) ₆ ²⁻	Na ⁺	0.04 ± 0.08 ^b
Ca ₃ [Zr(OH) ₆] ⁴⁺	Cl ⁻	0.48 ± 0.12 ^b
Ca ₄ [Th(OH) ₈] ⁴⁺	Cl ⁻	-0.01 ± 0.10 ^b

^a NEA-TDB.² ^b Present work (see text). ^c Derived from log γ_{OH^-} in 0–5 M CaCl₂ (based on the widely accepted set of Pitzer parameters reported by Harvie et al.¹⁴).

to pH 14 show no solubility increase at high pH; no indication for the formation of anionic thorium(IV) hydroxide complexes with five or six OH⁻ ligands is observed.²³ We conclude, as in the case of Zr^{IV}, that the complex formed in an alkaline CaCl₂ solution must also be stabilized by interaction with Ca²⁺ ions. The thorium concentrations measured after 14 and 27 days in selected samples in 2.0 M Ca(ClO₄)₂⁶ are also comparable to those in 2.0 M CaCl₂.

Note that the highest Th^{IV} concentration at pH_c = 12.2 in 4.5 M CaCl₂ (this sample is prepared particularly for EXAFS analysis) is measured after only 1 day of equilibration because the matrix solution is metastable at this high pH_c. Within the time of investigation, calcium hydroxychloride does not precipitate in this sample. The matrix solution is prepared by equilibration of 4.5 M CaCl₂ with Ca(OH)₂(cr) for 2 h. The solid Ca(OH)₂(cr) is removed before it starts to transform into less soluble calcium hydroxychloride (Ca₄(OH)₆Cl₂·13H₂O(cr) and/or Ca₂(OH)₂Cl₂·H₂O(cr)), which would lead to a lower pH_c value. At pH_c = 11.8 (in a matrix solution equilibrated for about 1 week), the solubility of ThO₂·xH₂O(s) is about 1.6 log units lower than that at pH_c 12.2. This is a thorium concentration that is not sufficient for EXAFS measurement. The H⁺ concentrations measured in 0.1–4.5 M CaCl₂ solutions in equilibrium with Ca(OH)₂(cr) agree well with the values calculated for these conditions using the widely accepted thermodynamic data and parameters reported by Harvie et al.¹⁴

3.3. Thermodynamic Model for the Solubility of Zr^{IV} and Th^{IV} in Alkaline CaCl₂ Solutions. The following section gives a brief summary of the thermodynamic model for the solubility of Zr^{IV} and Th^{IV} in alkaline solutions. In order to obtain standard-state equilibrium constants (*I* = 0, 25 °C), the specific ion interaction theory (SIT) recommended in the NEA-TDB reviews^{2,3} is used for ionic strength corrections. The SIT describes activity coefficients γ_i of aqueous species *i* by a Debye–Hückel term [$D = 0.509I_m^{1/2}/(1 + 1.5I_m^{1/2})$ at 25 °C, where *I_m* is the molal ionic strength] and specific interaction coefficients ϵ_{ij} for pairs of oppositely charged ions. The SIT coefficients used in the present study are listed in Table 2.

The solubility data at pH_c > 13 in 1.0 M NaClO₄–NaOH, in 0.5, 1.0, and 3.0 M NaCl–NaOH, and in pure 0.5–10 M NaOH can be described by the dissolution reaction



with log $K^\circ_{s,6} = -5.5 \pm 0.2$ and $\epsilon(\text{Zr(OH)}_6^{2-}, \text{Na}^+) = 0.04 \pm 0.08 \text{ kg}\cdot\text{mol}^{-1}$. The concentration of the complex Zr(OH)_6^{2-} in 0.5 M NaCl ($I = m_{\text{Cl}} = 0.5 \text{ mol}\cdot\text{kg}^{-1}$) is about 4 orders of magnitude lower than the zirconium concentrations at the same pH_c value in 0.2 M CaCl₂ with similar ionic strength and chloride concentration ($I = 0.6 \text{ mol}\cdot\text{kg}^{-1}$; $m_{\text{Cl}} = 0.4 \text{ mol}\cdot\text{kg}^{-1}$). Such a large difference at relatively low ionic strength cannot be explained by differences in the interaction parameters $\epsilon(\text{Zr(OH)}_6^{2-}, \text{Na}^+)$ and $\epsilon(\text{Zr(OH)}_6^{2-}, \text{Ca}^{2+})$. The experimental data can only be described by equilibria involving Ca²⁺ ions and the formation of ternary complexes $\text{Ca}_n[\text{Zr(OH)}_6]^{2n-2}$. An attempt to describe the experimental solubility data with the assumption that one Ca²⁺ ion ($n = 1$) is coordinated to $[\text{Zr(OH)}_6]^{2-}$ fails. When we assume $n = 2$ to describe the data, the solubility data in 2.0 M CaCl₂ must be excluded to obtain a reasonable fit. The calculation for $n = 3$ (in agreement with $N_{\text{Ca}} = 3$ determined by EXAFS; cf. section 3.4)



yields log $K^\circ_{s,6-3} = 0.7 \pm 0.3$ and $\epsilon(\text{Ca}_3[\text{Zr(OH)}_6]^{4+}, \text{Cl}^-) = 0.48 \pm 0.12 \text{ kg}\cdot\text{mol}^{-1}$ and describes all experimental solubility data in 0.1, 0.2, 0.5, 1.0, and 2.0 M CaCl₂ reasonably well (solid lines in Figure 1; the data in 0.1 and 1.0 M CaCl₂ are omitted for clarity).

Similarly, the solubility data for thorium(IV) hydroxide is well described if the number of Ca²⁺ ions associated with $[\text{Th(OH)}_8]^{4-}$ is assumed to be 4 or 5. Because the formation of a complex $\text{Ca}_5[\text{Th(OH)}_8]^{6+}$ seems unrealistic for reasons of symmetry and high charge, the value of $N_{\text{Ca}} = 4$ determined by EXAFS (cf. section 3.5) is adopted. The increase of the solubility in alkaline CaCl₂ solutions is then described by the reaction



with log $K^\circ_{s,8-4} = 1.8 \pm 0.5$ and $\epsilon(\text{Ca}_4[\text{Th(OH)}_8]^{4+}, \text{Cl}^-) = -0.01 \pm 0.10 \text{ kg}\cdot\text{mol}^{-1}$. We emphasize that these values for the thorium complex, in particular the interaction coefficient, depend strongly on the data in 4.5 M CaCl₂, i.e., at $I = 15.8 \text{ mol}\cdot\text{kg}^{-1}$, which is far above the validity range of SIT. The calculated thorium concentrations are shown as solid lines in Figure 2. Further solubility data and a more detailed discussion of the thermodynamic model will be published elsewhere.⁶

3.4. EXAFS Study of Zr^{IV} in Alkaline CaCl₂ Solutions. The *k*³-weighted EXAFS $\chi(k)$ functions of the zirconium samples and their corresponding Fourier transforms (FTs) are shown in Figure 3. The FT spectra exhibit a strong first peak at around 1.7 Å, corresponding to a phase-corrected value of approximately 2.2 Å, which originates from the first oxygen coordination shell surrounding the absorbing Zr^{IV} atoms. All four FT spectra show a second-shell contribution at around 2.9 Å, corresponding to a 3.4 Å phase-corrected distance. The pronounced second backscattering shell is also evident in the $\chi(k)$ functions, which appears as the superposition of two dampened sinusoidal waves. The higher frequency contribution is clearly visible from $k = 7 \text{ \AA}^{-1}$ upward.

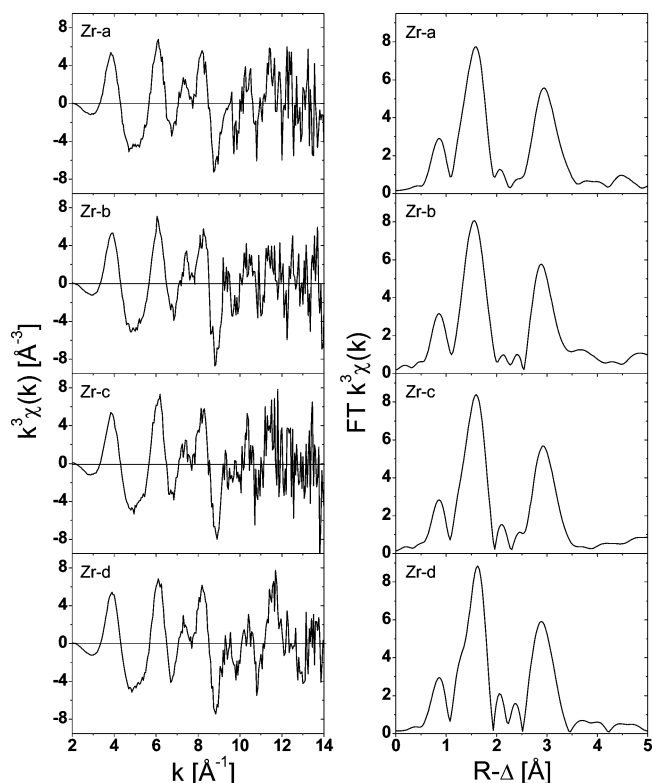


Figure 3. k^3 -weighted $\chi(k)$ Zr K-EXAFS of Zr^{IV} in alkaline $CaCl_2$ solutions (left panel) and corresponding FT magnitude spectra (right panel). See Table 1 for sample ID descriptions.

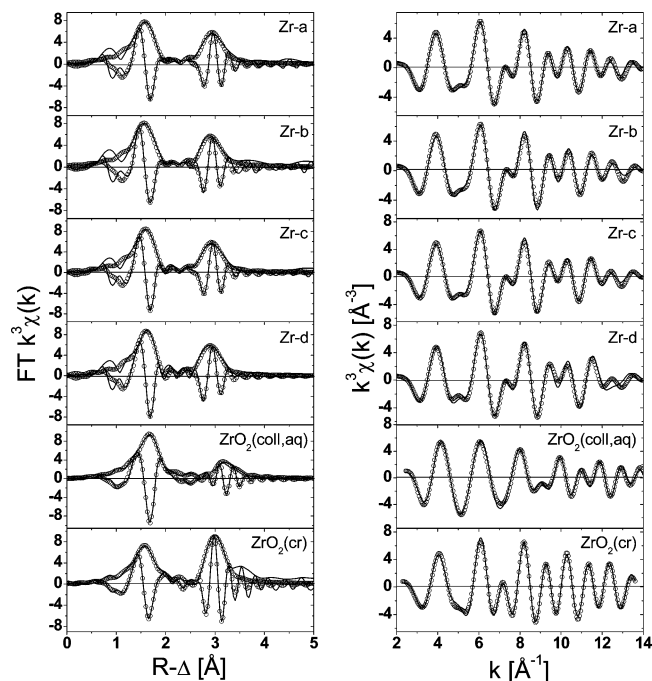


Figure 4. Fit results in R space (left panel) and corresponding back-transformed data (right panel) for Zr^{IV} in alkaline $CaCl_2$ solutions. Data are depicted as solid lines and the fits as open circles. Analysis of a solution containing microcrystalline $ZrO_2 \cdot xH_2O$ colloids and solid monoclinic $ZrO_2(cr)$ presented in ref 11 is shown for comparison.

Fits to the FT spectra and their corresponding back-transformed $\chi(k)$ functions are depicted in Figure 4. Metrical parameters obtained in the fits are summarized in Table 3. The first-shell contribution in all samples is modeled by a

Table 3. Metrical Parameters Extracted by Least-Squares Fit Analysis of the Zirconium Samples EXAFS Spectra Shown in Figure 4

ID	shell	R (Å)	N	σ^2 (Å ²)	ΔE (eV)	R factor ^a
Zr-a	O	2.21(2)	6.8(8)	0.008(1)	-8.5(2.8)	0.017
	Ca	3.39(1)	2.6(4)	0.002(1)	6.4(1.4)	
Zr-b	O	2.22(1)	7.2(9)	0.008(1)	-8.5(3.0)	0.027
	Ca	3.37(1)	2.4(5)	0.002(1)	5.1(1.9)	
Zr-c	O	2.20(1)	6.5(6)	0.007(1)	-8.5(3.0)	0.016
	Ca	3.39(1)	2.7(4)	0.003(1)	6.2(1.3)	
Zr-d	O	2.18(2)	5.8(9)	0.005(1)	-10.6(4.1)	0.036
	Ca	3.38(1)	3.1(8)	0.004(2)	5.3(2.1)	

^a The R factor describes the overall goodness of fit, which is χ^2 divided by the degrees of freedom. A value that equals 0.03 means that theory and data agree within 3%.

single oxygen shell of 5.8–7.2 atoms at 2.18–2.22 Å. Taking into account the approximate 20% uncertainty in EXAFS analysis for coordination numbers, these values are interpreted to reflect the presence of six OH^- ligands. The H atoms are not detected by EXAFS because of their low backscattering ability. The Debye–Waller factor values (0.005–0.008 Å²) indicate variation in the Zr–O distances. Attempts to apply a model of two separate oxygen shells do not improve the fit results.

Evaluation of the second-shell feature deserves more detailed discussion. A second shell attributed to a Zr–Zr distance in polynuclear zirconium(IV) hydroxide complexes present in acidic aqueous Zr^{IV} solutions is reported in our previous study by Cho et al.¹¹ In that investigation, reference spectra of solid monoclinic $ZrO_2(cr)$ and an aqueous sample containing microcrystalline $ZrO_2 \cdot xH_2O$ colloids, $ZrO_2(coll, aq)$, whose structure is described to consist of tetrameric $[Zr_4(OH)_8(H_2O)_{16}]^{8+}$ units, are presented. The spectra are reproduced in Figure 4. Further samples that we can consider as references with Zr–Zr distances are reported by Hagfeldt et al. with $R_{Zr-Zr} = 3.588(2)$ Å in the solvated tetrameric $[Zr_4(OH)_8(H_2O)_{16}]^{8+}$ aqueous complex¹³ and by Walther et al. with $R_{Zr-Zr} \geq 3.7$ Å in a series of 1.5×10^{-3} M Zr^{IV} in hydrochloric acid at $0 < pH_c < 1.2$.¹² The FT magnitudes of reference EXAFS spectra exhibit two main FT peaks, similar to the spectra of samples Zr-a through Zr-d shown in Figure 3. However, the second FT shell in the reference FT spectra is shifted to longer interatomic distances, and the imaginary part of their FT differs from those of our Zr^{IV} in alkaline $CaCl_2$ solutions. This difference in the imaginary part indicates that the second FT peak is associated with different photoelectron phase shifts, i.e., with different atom types in these two systems. The FT imaginary part of the first FT peak is similar in all spectra shown in Figure 3, including reference spectra, because this peak is associated with oxygen backscattering atoms in all cases. The FT imaginary part of the second shell peaks at the low $R-\Delta$ flank of the FT magnitude maximum in our alkaline $CaCl_2-Zr^{IV}$ solution spectra. The FT imaginary part of the second FT peak for the two reference spectra shows a different pattern, showing that it is associated with backscattering atoms of different types. It is therefore not surprising that all attempts to fit the solution data in Figure 3 using a model of zirconium as the backscattering atom type for the second coordination shell do not lead to reliable fit results; either

coordination numbers become negative or, when N is held constant in the fit routine, distances obtained are too small to make any physical sense. Therefore, we can rule out with confidence the presence of polynuclear colloidal hydrolysis species. This is in accordance with the solubility data as a function of the total metal concentration. No change in the solubility curve slope ($\log [\text{Zr}]$ vs pH_c) is observed with increasing calcium concentration. This is in contrast to what one would expect from the associated shift in the polynuclear species equilibrium concentration. The curves are simply shifted to higher values with increasing calcium concentration, while retaining their slope of 2. This means that the dominant solution species is a distinct mononuclear complex; no polynuclear hydrolysis species or polymeric species with bridging Ca or Zr atoms are present. Fits assuming Cl atoms as backscattering atoms in the second shell are also attempted without success. There are no chloride ligands present in the zirconium complexes.

We can successfully model the second coordination sphere for sample Zr-a through Zr-d spectra using solely Ca as backscattering atoms. Fits using Ca atoms yield distances of 3.37–3.39 Å and coordination numbers of 2.4–3.1, i.e., three Ca atoms considering the fit accuracy and rounding to the next integer. The Debye–Waller factors of the second shell are small (0.002–0.004 Å²) compared to values of 0.005–0.012 Å² associated with Zr–Zr distances reported for colloidal zirconium(IV) hydroxide species.¹¹ This is an indication that well-defined species are present, as opposed to mixtures of different species. We interpret this as the first indication of Ca²⁺ ions being bound to edges of the zirconium coordination polyhedron because this coordination mode is more rigid and would therefore likely have a small EXAFS Debye–Waller factor.

The number of ligating hydroxyl groups derived both from the pH dependence of the solubility (slope 2 for $\log [\text{Zr}]_{\text{tot}}$ vs pH_c) and from EXAFS analysis for the aqueous ternary Ca–Zr^{IV}–OH complex is six; the number of calcium ions associated with the complex is determined from the EXAFS analysis to be three. In our development of a structural model for the Ca₃[Zr(OH)₆]⁴⁺ solution complex, we first assume an octahedral geometry for the 6-fold-coordinated Zr⁴⁺ ion. This is the expected geometry based on the minimization of ligand repulsion forces. We further assume that the Ca²⁺ ions are bound to the edges of the octahedron. We stress here that we are describing an idealized structure and distortion from this idealized representation presumably occurs. If we calculate the Zr–O–Ca bond angle in the Ca₃[Zr(OH)₆]⁴⁺ complex using the Zr–O and Zr–Ca interatomic distances obtained from EXAFS analysis ($R_{\text{Zr–OH}} = 2.20 \pm 0.02$ Å and $R_{\text{Zr–Ca}} = 3.38 \pm 0.02$ Å), we obtain 100°. This angle is the same as that for the chains of edge-linked octahedra present in the rutile structure.²⁹ However, the Zr–O distance in the complex is longer than one would expect for a rutile-like structured complex. Using the Ti–O distance in the TiO₂(cr) rutile structure ($R_{\text{Ti–O}} = 1.96$ Å) and taking into account the differing cation radii of Ti⁴⁺ and Zr⁴⁺ ions,

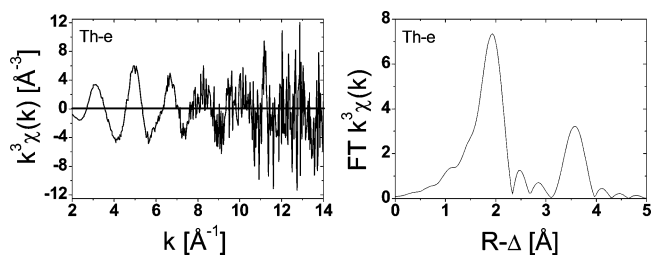


Figure 5. k^3 -weighted $\chi(k)$ Th L3-EXAFS of 3×10^{-3} M Th^{IV} in 4.5 M CaCl₂ at $\text{pH}_c = 12.2$ (left panel) and corresponding FT magnitude spectra (right panel).

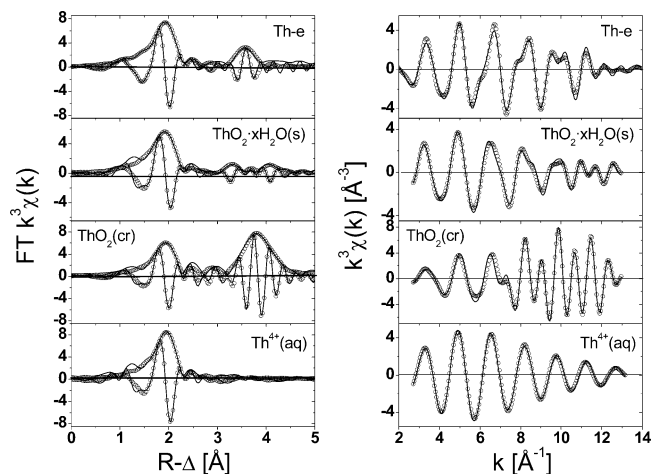


Figure 6. Fit results in R space (left panel) and for the corresponding back-transformed data (right panel) of the Th^{IV} sample in an alkaline CaCl₂ solution. Data are depicted as solid lines and fit curves as open circles. Analysis of a microcrystalline ThO₂· x H₂O(s) sample and crystalline anhydrous ThO₂(cr) in ref 10 and Th⁴⁺ in an acidic aqueous solution presented in ref 9 is shown for comparison.

$r(\text{Ti}^{4+}; N_{\text{O}}=6) = 0.61$ Å and $r(\text{Zr}^{4+}; N_{\text{O}}=6) = 0.72$ Å,³⁰ we would expect $R_{\text{Zr–OH}} = 2.07$ Å for a rutile-like structure. This is more than 0.1 Å shorter than the observed $R_{\text{Zr–OH}} = 2.20 \pm 0.02$ Å and indicates that our complex might have a coordination number of $N_{\text{O}} = 7–8$; i.e., the complex might include one or two H₂O ligands.

3.5. EXAFS Study of Th^{IV} in Alkaline CaCl₂ Solutions.

The k^3 -weighted EXAFS $\chi(k)$ function sample Th-e and its corresponding FT are shown in Figure 5. The FT spectrum is dominated by a strong first oxygen shell contribution at 1.9 Å [phase-corrected $R(\text{O}) \sim 2.5$ Å] and a second-shell contribution at around 3.7 Å (~ 4 Å phase corrected). A qualitative comparison of this FT spectrum with that for the Th⁴⁺(aq) ion^{4,9,10} clearly shows the presence of a different species in our solution. The magnitude of the sample Th-e second shell is significantly greater than those reported for microcrystalline ThO₂· x H₂O(s) and polynuclear thorium(IV) hydroxide colloids in an acidic NaCl solution but lower than that for crystalline anhydrous ThO₂(cr).¹⁰

Fits to the experimental FT spectrum and the corresponding back-transformed $\chi(k)$ function are shown in Figure 6. Metrical parameters obtained in theoretical fits to the data are listed in Table 4. The first FT peak is well fit by a single oxygen shell. The coordination number of 8.6 ± 1.2 oxygen atoms at 2.47 Å is consistent with a model of eight OH[–]

(29) Gonschorek, W. Z. *Kristallogr.* **1982**, *160*, 187–203.

(30) Shannon, R. D. *Acta Crystallogr., Sect. A* **1976**, *32*, 751–767.

Table 4. Metrical Parameters Extracted by Least-Squares Fit Analysis of the Thorium Sample (Th-e) EXAFS Spectrum in Figure 6

ID	shell	R (Å)	N	σ^2 (Å ²)	ΔE (eV)	R factor
Th-e	O	2.47(3)	8.6(1.2)	0.007(1)	4.0(3.0)	0.019
	Ca	3.98(2)	3.8(5)	0.005(1)	12.0(2.4)	

ligands expected from the observed solubility dependencies on pH and CaCl₂ concentration. Similar to Zr^{IV} in alkaline CaCl₂ solution samples, the second-shell contribution is clearly different from the previously reported experimental data of microcrystalline ThO₂·xH₂O(s), crystalline anhydrous ThO₂(cr), and Th⁴⁺ in 1.5 M HClO₄.^{4,9,10} and is well modeled with calcium as the backscattering atom. Good agreement between the data and model is obtained with $N_{\text{Ca}} = 3.8$, i.e., four Ca atoms in the second coordination sphere, at a distance of 3.98 Å.

Fits assuming thorium as backscattering atoms are also performed as a cross-check, but neither stable nor physically meaningful results are obtained. We also tried to model the second-shell EXAFS using chloride ions, again without obtaining meaningful results. We can safely exclude the presence of any polynuclear hydrolysis species, in accordance with solubility data, as well as the presence of any coordinating chloride ions.

The coordination numbers and interatomic distances derived from the EXAFS analysis for the Ca₄[Th(OH)₈]⁴⁺ complex indicate that the coordination of this complex is similar to that of the fluoride structure in crystalline ThO₂(cr). The distance $R_{\text{Th-OH}} = 2.47 \pm 0.03$ Å in our aqueous complex is 0.05 Å longer than $R_{\text{Th-O}}$ in ThO₂(cr) (EXAFS,¹⁰ 2.41 ± 0.02 Å; XRD,³¹ 2.42 Å). However, the $R_{\text{Th-Ca}} = 3.98 \pm 0.02$ Å distance in Ca₄[Th(OH)₈]⁴⁺ is equal to $R_{\text{Th-Th}}$ in ThO₂(cr) (EXAFS,¹⁰ 3.98 ± 0.02 Å; XRD,³¹ 3.96 Å). This observation is consistent with the similar ionic radii of the Ca²⁺ and Th⁴⁺ ions, $r(\text{Ca}^{2+}; N_{\text{O}}=6) = 1.00$ Å and $r(\text{Th}^{4+}; N_{\text{O}}=8) = 1.05$ Å.³⁰ The large σ^2 values for the Th–O shell suggest that the polyhedron of this aqueous

complex is most likely distorted. Taking into account the uncertainty in $N_{\text{O}} = 8.6 \pm 1.2$ and the fact that the observed distance $R_{\text{Th-O}} = 2.47 \pm 0.03$ is about 0.05 Å longer than that in ThO₂(cr) but close to the that of 10-fold-coordinated Th⁴⁺ aquo ion⁹ ($R_{\text{Th-O}} = 2.45 \pm 0.01$ Å) and Th(CO₃)₅⁶⁻ solution species^{32,33} ($R_{\text{Th-O}} = 2.50 \pm 0.02$ Å), we cannot exclude that our complex has a coordination number of $N_{\text{O}} = 9-10$, with one or two additional H₂O ligands.

4. Concluding Remarks

We have identified a new type of ternary Ca–M^{IV}–OH complex, where anionic metal(IV) hydroxide complexes are stabilized by the association/ion-pair formation with Ca²⁺ ions, and characterized them by EXAFS. The complex stoichiometries of Ca₃[Zr(OH)₆]⁴⁺ and Ca₄[Th(OH)₈]⁴⁺ obtained by EXAFS are consistent with the observed dependencies of Zr^{IV} and Th^{IV} solubilities on pH and CaCl₂ concentration. The only types of similar complexes reported in the literature are ternary Ca–U^{VI}–CO₃ complexes, Ca[UO₂(CO₃)₃]²⁻ and Ca₂[UO₂(CO₃)₃]⁰, which have been studied in NaClO₄ and NaHCO₃ solutions containing 10⁻³–10⁻² M Ca²⁺ mainly by time-resolved laser-induced fluorescence spectroscopy^{34–37} but also by EXAFS.^{35,37} Possibly, the stabilization of anionic hydroxide and carbonate complexes by Ca²⁺ ions is a more general phenomenon that deserves further investigation. The presence of such species can have a significant impact on the solubility and aqueous speciation of actinide ions.

IC070318T

(31) Magini, M.; Cabrini, A.; Scibona, G.; Johansson, G.; Sandström, M. *Acta Chem. Scand. A* **1976**, *30*, 437–447.

- (32) Felmy, A. R.; Rai, D.; Sterner, S. M.; Mason, M. J.; Hess, N. J.; Conradson, S. D. *J. Solution Chem.* **1997**, *26*, 233–248.
- (33) Altmaier, M.; Neck, V.; Denecke, M. A.; Yin, R.; Fanghänel, Th. *Radiochim. Acta* **2006**, *94*, 495–500.
- (34) Bernhard, G.; Geipel, G.; Brendler, V.; Nitsche, H. *Radiochim. Acta* **1996**, *74*, 87–91.
- (35) Bernhard, G.; Geipel, G.; Reich, T.; Brendler, V.; Amayri, S.; Nitsche, H. *Radiochim. Acta* **2001**, *89*, 511–518.
- (36) Kalmykov, S. N.; Choppin, G. R. *Radiochim. Acta* **2000**, *88*, 603–606.
- (37) Kelly, S. D.; Kemner, K. M.; Brooks, S. C. *Geochim. Cosmochim. Acta* **2007**, *71*, 821–834.